



Research Paper

Domestic thermoelectric cogeneration system optimization analysis, energy consumption and CO₂ emissions reductionHassan Jaber^a, Mohamad Ramadan^a, Thierry Iemenand^b, Mahmoud Khaled^{a,c,*}^a Energy and Thermo-Fluid Group, School of Engineering, International University of Beirut BIU, Beirut, Lebanon^b LARIS EA 7315, ISTIA, University of Angers, Angers, France^c Univ Paris Diderot, Sorbonne Paris Cité, Interdisciplinary Energy Research Institute (PIERI), Paris, France

HIGHLIGHTS

- A domestic thermoelectric cogeneration system is suggested.
- The concept is drawn and the corresponding thermal modeling is developed.
- An optimization analysis is carried out using the thermal modeling.
- Results show that water can be heated to up to 97 °C.
- When TEGs are placed at the pipe inner wall, the concept is the most cost-effective.

ARTICLE INFO

Article history:

Received 11 September 2017

Revised 16 October 2017

Accepted 27 October 2017

Available online 7 November 2017

Keywords:

Carbon dioxide emission
 Domestic hot water
 Energy consumption
 Domestic thermoelectric cogeneration system
 Heat recovery
 Optimization
 Thermal modeling

ABSTRACT

In this paper, a domestic thermoelectric cogeneration system (DCS) is suggested. This system permits to use the lost heat of exhaust gases to simultaneously heat water and produce electricity via thermoelectric generators (TEG). To proceed, the concept of the system is drawn and the corresponding thermal modeling is developed. An optimization analysis, based on the position of the thermoelectric generators within the system, is carried out using the thermal modeling. The TEGs are placed on the inner or outer walls of the tank or the pipe (cases 2–5), or on all of them (case 6). Results show that water can be heated to up to 97 °C, when TEGs are located on the inner wall of the tank. More the TEGs are nearer to the exhaust gases, higher is the total power produced by the TEGs and lower is the water temperature. The power produced by one TEG in direct contact with the exhaust gases is 0.35 W and the water temperature is 76 °C. Also, a DCS with TEG located at all layers can generate up to 52 W and 81 °C hot water, however this configuration has high initial cost. An economic and environmental concerns are considered. Results show that DCS with TEGs located on the inner wall of the pipe has a payback period of 1 year and 8 months when water is heated 60 times per month. In addition to that, it was shown that the location of TEGs do not affect the amount of CO₂ gas reduced which is about 6 tons yearly. Finally, this study shows that the configuration where TEGs are placed at the inner wall of the pipe is the most cost-effective energy recovery configuration.

© 2017 Elsevier Ltd. All rights reserved.

1. Introduction

1.1. Background

The driving forces to seek new sources of energy are energy depletion, high cost of energy, and strict laws related to energy issued by governments. World population has a growth rate of

1.2% with an expected increase in population to 8.9 billion in 2050 and it certainly indicates to a high and growing rate in the demand on energy. Energy management, sustainability and renewable energy are excellent solutions envisaged to remedy to the energy increase since the new adopted solutions need to be sustainable in order to meet energy demand of future generations.

Renewable energy, which includes solar, wind, wave, biomass, and others, is being an effective new source of energy nowadays [1–5]. However, this source is facing some limitations related to its availability, location, low efficiency, high initial cost, and other

* Corresponding author at: Energy and Thermo-Fluid Group, School of Engineering, International University of Beirut BIU, Beirut, Lebanon.

E-mail address: mahmoud.khaled@liu.edu.lb (M. Khaled).

Nomenclature

A	area [m ²]	conv,air	convection between air and tank's wall
h	convection heat transfer coefficient [W/m ² K]	conv,i	convection between gases and pipe's surface
ρ	density [kg/m ³]	conv,w-p	convection between water and pipe's surface
q	heat transfer rate [W]	conv,w-w	convection between water and tank's wall
L	length of the tank [m]	g	gases
m	mass [kg]	H	hot
N	number of items	p,i	inner pipe
P	power produced [W]	w,i	inner tank wall
$P_{1\text{ TEG}}$	power produced by one TEG [W]	p,o	outer pipe
r	radius [m]	w,o	outer tank wall
T_a	temperature [°C]	p	pipe
ΔT	temperature difference at the sides of the TEG [°C]	sur,Pi	pipe inner surface
k	thermal conductivity [W/m K]	sur,Po	pipe outer surface
R	thermal resistance [K/W]	wall,i	tank wall inner surface
e	thickness of the TEG [m]	wall,o	tank wall outer surface
V	volume [m ³]	TEG	thermoelectric generator
		w	water
Subscripts			
a	ambient		
c	cold		

major limitations that makes researchers vigilant in the implementation.

Energy management is a technique implemented actually to assist renewable energies [6–9]. This technique is highly related to finding ways of enhancing the way of using energy and/or recovering lost energy. Many residential and industrial applications depend on thermal energy, in which part of this energy is being used and the other is dumped in environment without taking advantage of it. This thermal energy lost can be dumped either by exhaust gases, or cooling air, or cooling water. Heat recovery can be applied on many applications with different methods for a variety of recovery purposes. Jaber et al. [10] presented a review on heat recovery systems classifying them according to the quality of energy lost (temperature of gases), equipment used, and purposes of the heat recovery. Heat recovery purposes could be for generating electricity, heating, cooling, or storing energy for a later use, or even by a combination of more than one purpose as a hybrid heat recovery system.

1.2. Heat recovery from exhaust gases

Heat lost in mechanical systems is usually through exhaust gases as in boilers [11–14], heat pump [15,16], industrial furnace [17,18], generators [19–21], internal combustion engines (ICE) [22–28], chimneys [29,30], and other applications [31–35] or by heating, ventilating, and air conditioning (HVAC) systems [36,37], and hot water [38–42]. Hossain and Bari [43] performed an experimental study on heat recovery from exhaust gases of a 40 kW diesel generator using different organic fluids. In a shell and tube heat exchanger, water, ammonia and HFC 134a were utilized as working fluids. Results show that using water can produce 10% additional power compared to ammonia (9%) and HFC 134a (8%). Prabu and Asokan [44] carried out a study of heat recovery from ICE using phase change material. It was shown that about 4–7% of the heat lost was recovered, and the maximum energy saved at full load in thermal storage tank achieved 0.5 kW. In addition, the heat recovery process suggested can be enhanced by increasing the effective area of the heat recovery heat exchanger. Najjar et al. [45] presented a heat recovery system applied to gas turbine in order to cool inlet air temperature to the turbine engine. Two cycles were constructed: the first cycle permits to produce power

by propane organic Rankine cycle which will be used in the second cycle; the second cycle is a gas refrigeration cycle used to cool the air entering the turbine engine. It was found that 35% and 50% increase in the net power and overall efficiency were achieved respectively, by dropping the inlet air temperature 15 °C. Economical study showed that about two years are required to payback the project. Gao et al. [46] performed a review on heat recovery from stoves using thermoelectric generators (TEG). Thermoelectric generators are utilized to drive a fan that pushes air to the furnace, optimizing the air to fuel ratio which improved combustion efficiency. TEGs can also be used to power a light or radio or other low electric consuming machines. Khaled et al. [30] carried out an experimental study about heat recovery from exhaust gases of a chimney for generating domestic hot water. Results show that by one hour temperature of water increased 68 °C, and 70% of the heat gain by water was from the bottom side of the prototype used (heat transfer by convection and radiation).

1.3. Power generation using thermo-electricity

Many studies were performed on thermoelectric generators [47–51]. Jang and Tsai [52] performed a parametric study for the thermal and electrical properties of thermoelectric module utilizing waste heat experimentally and numerically. The effect of changing the size of spreader was studied to show that when using a proper size of the spreader the thermal resistance decreases and the maximum total power increases (up to 50%). Lu et al. [53] carried out a numerical study on the effect of heat enhancement for exhaust gases on the performance of thermoelectric generators. Two types of heat transfer enhancements (rectangular offset-strip fins and metal foams) are investigated. Results show that metal foam with low porosity would maximize the power produced by TEG more than the rectangular offset-strip. Navarro-Peris et al. [54] presented a study about producing electricity by TEGs that utilized heat lost from a compressor, which increases the efficiency of refrigeration and heat pump system. An experimental study was carried out varying the heat sink type. Low power was produced when the system is cooled naturally (natural convection), around 80 W/m² and when the heat sink is subjected to forced convection the power per area increased to 280 W/m² with an increase in temperature difference (44 °C). When cooled

water was utilized as heat sink temperature, the power produced increased up to 1180 W/m^2 . Ma et al. [55] performed a theoretical study on heat recovery from biomass gasifier using thermoelectric generators. The outlet temperature from the gasifier is up to $500 \text{ }^\circ\text{C}$. A thermoelectric generator system composed of eight thermoelectric modules is utilized to recover this lost heat. Results showed that the maximum total power produced is 6.1 W with a power density of 193 W/m^2 .

1.4. Motivation

As shown in the literature review presented above, considerable researches are devoted to heat recovery from exhaust gases and power generation using thermoelectric modules. Scarce are the studies that couple between these two energy research fields [56–58]. In this context, the present work suggests a new concept that permits to simultaneously heat water and generate electrical power, as a domestic thermoelectric cogeneration system. To proceed, the concept of the system is drawn and the corresponding thermal modeling is developed. An optimization analysis, based on the position of the thermoelectric generators within the system, is carried out using the thermal modeling. Finally, economic and environmental concerns are considered. It was shown that the configuration where TEGs are placed at the inner wall of the pipe is the most cost-effective energy recovery configuration.

2. Domestic thermoelectric cogeneration system

This section is devoted to the description of the suggested Domestic Thermoelectric Cogeneration System (DTCS). This system is a hybrid heat recovery system utilized to generate domestic hot water and produce electricity from the exhaust gases known as domestic thermoelectric cogeneration system (DTCS). The goal of this hybrid heat recovery system is to heat water mainly and then produce electric power as much as possible (Fig. 1).

Exhaust gases that pass through a pipe release its thermal energy to water that surrounds the pipe located inside a cylindrical tank. At the same time, electricity is produced by thermoelectric generators located as a cylindrical layer over a surface. The main aim from this study is to make a comparison between the temperature of the water and the power produced by TEGs by changing the location of the thermoelectric generators. The location of the thermoelectric generators can be inside or outside the wall of the pipe or inside or outside the wall of the cylindrical tank, or even located at all sides of the pipe and the cylindrical tank. Fig. 2 shows a heat recovery system that generates water heating. Such system will be improved by adding TEGs either on the surfaces of the pipe or the tank in their inner and outer side, or at all positions. Such hybrid heat recovery system can be coupled with many industrial and residential applications that generates high amount of exhaust gases or even relatively low amount of exhaust gases (Fig. 3). Gas or steam power plants, diesel power plants, industrial furnace (glass, steel furnace...), power generators, internal combustion engines, chimneys are applications capable to be coupled with

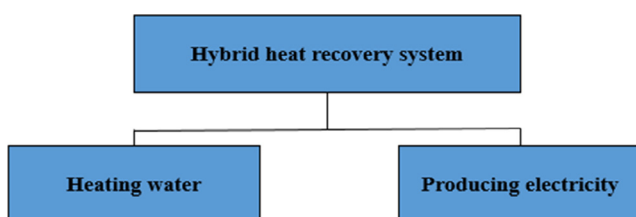


Fig. 1. Hybrid heat recovery goals.

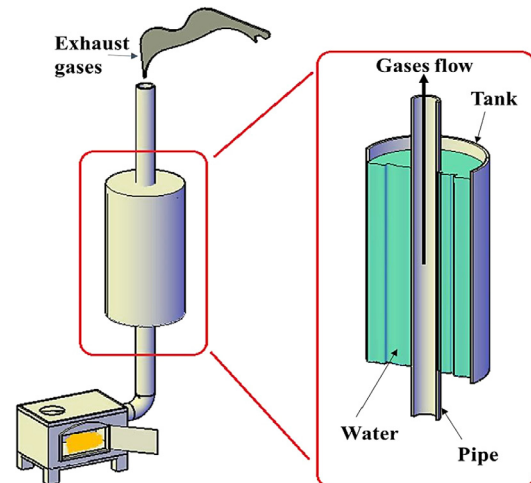


Fig. 2. Heat recovery system.

the hybrid heat recovery system. In this study the domestic thermoelectric cogeneration heat recovery system will be implemented on a chimney, in which exhaust gases from the chimney are utilized to heat water and produce electricity via TEGs.

Six cases will be taken into consideration, the first is a simple heat recovery system utilized just to generate domestic hot water which will be the reference for other cases. The remaining cases are hybrid heat recovery systems in which the location of the TEG is changed. Table 1 shows each case and its corresponding TEGs location. Thermoelectric generators are passive devices used to generate electricity when they are sandwiched in a temperature difference [59]. In each of the hybrid cases [2–6], the heat source and heat sink is changed. In case 2, the heat source is the wall of the cylindrical tank and air is the heat sink, whereas in case 3 water is the heat source and cylindrical tank wall is the heat sink. In cases 4 and 5, the heat source is pipe wall and the exhaust gases respectively whereas the heat sink is the water and pipe wall respectively. Finally, case 6 is a combination of the previous cases 2, 3, 4, and 5.

3. Thermal modeling

A thermal modeling is done in order to obtain the water temperature and the power generated by the thermoelectric generators. It is assumed that the exhaust gases are of constant temperature and mass flow rate (steady state) and one dimensional heat flow. Steps required to calculate water temperature and power output is as follows:

1. Thermal modeling of each case in terms of thermal resistance.
2. Calculation of the total thermal resistance (R_{total}).
3. Calculation of the heat flow rate (q).
4. Calculation of the temperature at each point.
5. Calculation of the temperature difference at the surfaces of the TEG.
6. Calculation of the power generated by one TEG ($P_{1 \text{ TEG}}$).
7. Calculation of the number of TEG available (N_{TEG}).
8. Calculation of the total power produced by TEGs (P_{total}).

Starting by the thermal modeling, Table 2 shows the thermal modeling of each case in terms of thermal resistance where $T_{g,i}$, $T_{sur,pi}$, $T_{sur,po}$, T_w , $T_{wall,i}$, $T_{wall,o}$, T_a , T_H and T_c are the temperature of exhaust gases, inner pipe surface, outer pipe surface, water, inner cylindrical tank surface, outer cylindrical tank surface, ambient,

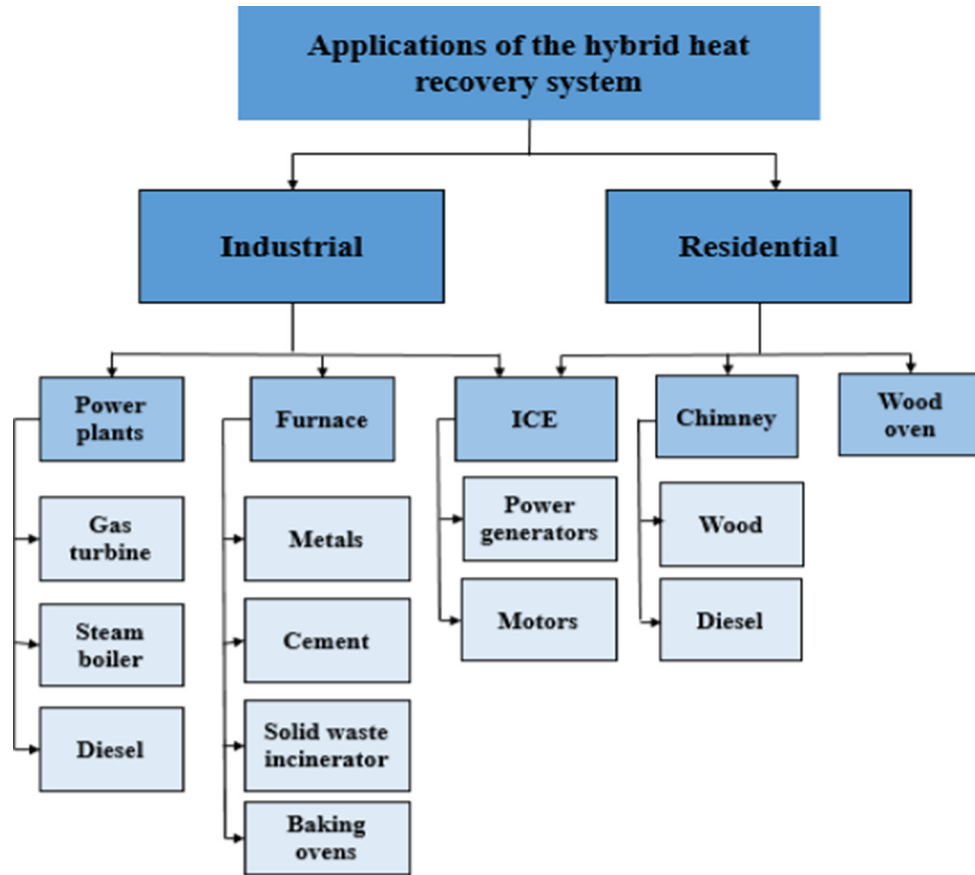


Fig. 3. Applications of the hybrid heat recovery system.

Table 1
Location of TEGs in each studied case.

Case number	TEG position	Thermal layers
1 (reference)	Without TEG	
2	At the outer radius of cylinder's wall	
3	At the inner radius of cylinder's wall	
4	At the outer radius of pipe's wall	
5	At the inner radius of pipe's wall	
6	At the inner and outer radius of the pipe and cylinder	

hot side of TEG, and cold side of TEG respectively. $R_{conv,i}$, R_p , $R_{conv,w-p}$, $R_{conv,w-w}$, R_{wall} , and $R_{conv,air}$, R_{TEG} are the thermal resistance of internal convection of gases in pipe, conduction in the pipe wall, convection between water and pipe, convection between water and cylindrical tank wall, conduction in the cylindrical tank wall, convection of tank with air, and conduction in thermoelectric generator respectively.

The heat flow rate (q) can be calculated with the following equation:

$$q = \frac{\Delta T}{R_{Total}} \tag{1}$$

where ΔT is the temperature difference between exhaust gases and ambient air:

$$\Delta T = T_{g,i} - T_a \tag{2}$$

and R_{Total} is the summation of the thermal resistance in each case, described below for the studied cases.

For case 1, Fig. 4 shows a cross section of the system where the temperature points are viewed.

$R_{conv,i}$, R_p , $R_{conv,w-p}$, $R_{conv,w-w}$, R_{wall} , and $R_{conv,air}$ are as follows:

$$R_{conv,i} = \frac{1}{h_g(2\pi r_{p,i}L)} \tag{3}$$


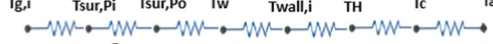


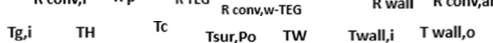
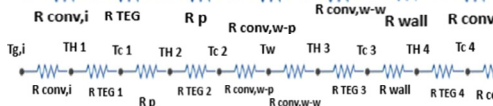
$$R_p = \frac{\ln \left[\frac{r_{p,o}}{r_{p,i}} \right]}{2\pi k_p L} \tag{4}$$

$$R_{conv,w-p} = \frac{1}{h_w(2\pi r_{p,o}L)} \tag{5}$$

$$R_{conv,w-w} = \frac{1}{h_w(2\pi r_{w,i}L)} \tag{6}$$

$$R_{wall} = \frac{\ln \left[\frac{r_{w,o}}{r_{w,i}} \right]}{2\pi k_w L} \tag{7}$$

Table 2
Thermal modeling of each case.

Case number	TEG position	Thermal equivalent circuit
1	Without TEG	$T_{g,i} \quad T_{sur,Pi} \quad T_{sur,Po} \quad T_w \quad T_{wall,i} \quad T_{wall,o} \quad T_a$ 
2	At the outer radius of cylinder's wall	$T_{g,i} \quad T_{sur,Pi} \quad T_{sur,Po} \quad T_w \quad T_{wall,i} \quad T_H \quad T_c \quad T_a$ 
3	At the inner radius of cylinder's wall	$T_{g,i} \quad T_{sur,Pi} \quad T_{sur,Po} \quad T_w \quad T_H \quad T_c \quad T_{wall,o} \quad T_a$ 
4	At the outer radius of pipe's wall	$T_{g,i} \quad T_{sur,Pi} \quad T_H \quad T_c \quad T_w \quad T_{wall,i} \quad T_{wall,o} \quad T_a$ 
5	At the inner radius of pipe's wall	$T_{g,i} \quad T_H \quad T_c \quad T_{sur,Po} \quad T_w \quad T_{wall,i} \quad T_{wall,o} \quad T_a$ 
6	At the inner and outer radius of the pipe and cylinder	$T_{g,i} \quad T_H 1 \quad T_c 1 \quad T_H 2 \quad T_c 2 \quad T_w \quad T_H 3 \quad T_c 3 \quad T_H 4 \quad T_c 4 \quad T_a$ 

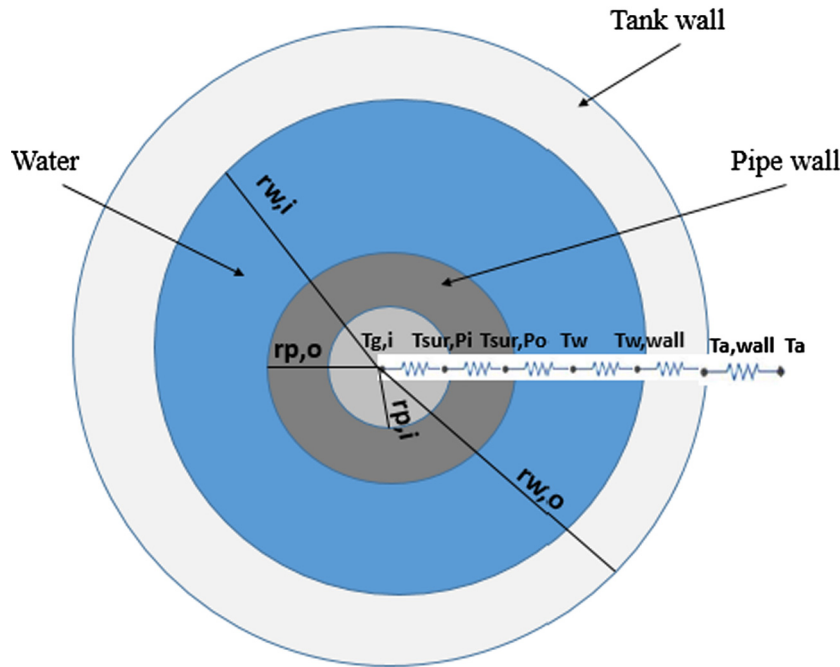


Fig. 4. Top cross sectional view of the cogeneration system in case 1.

$$R_{conv,air} = \frac{1}{h_a(2\pi r_{w,o}L)} \quad (8)$$

For case 2, Fig. 5 presents the top view of the tank, it shows the TEG layer at the outer surface of the tank.

$R_{conv,i}$, R_p , $R_{conv,w-p}$, $R_{conv,w-w}$ and R_{wall} are as case 1, whereas R_{TEG} and $R_{conv,air}$ are:

$$R_{TEG} = \frac{\ln \left[\frac{r_{w,o}+e}{r_{w,o}} \right]}{2\pi k_{TEG}L} \quad (9)$$

$$R_{conv,air} = \frac{1}{h_a(2\pi(r_{w,o} + e)L)} \quad (10)$$

For case 3, Fig. 6 shows the top view of the cylinder where the TEGs layer are located at the inner surface of the tank.

$R_{conv,i}$, R_p , $R_{conv,w-p}$, R_{wall} and $R_{conv,air}$ are as the reference case 1 whereas R_{TEG} and $R_{conv,w-w}$ are:

$$R_{TEG} = \frac{\ln \left[\frac{r_{w,i}}{r_{w,i}-e} \right]}{2\pi k_{TEG}L} \quad (11)$$

$$R_{conv,w-w} = \frac{1}{h_w(2\pi(r_{w,i} - e)L)} \quad (12)$$

For case 4, Fig. 7 presents a top cross section of the tank, TEGs are located at the outer surface of the pipe.

$R_{conv,i}$, R_p , $R_{conv,w-w}$, R_{wall} and $R_{conv,air}$ are as the reference case, whereas R_{TEG} and $R_{conv,w-p}$ are:

$$R_{TEG} = \frac{\ln \left[\frac{r_{p,o}+e}{r_{p,o}} \right]}{2\pi k_{TEG}L} \quad (13)$$

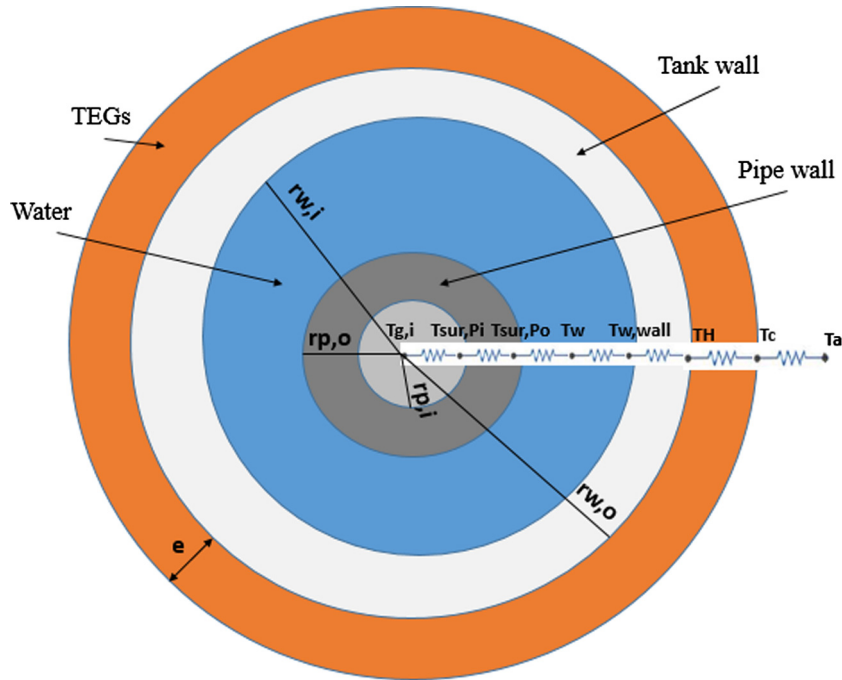


Fig. 5. Top cross sectional view of the cogeneration system in case 2.

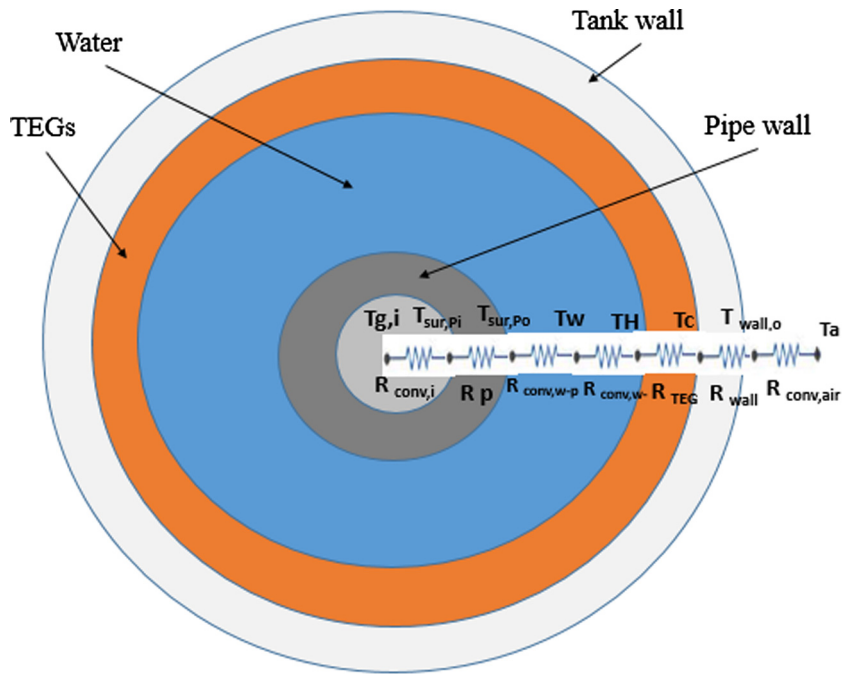


Fig. 6. Top cross sectional view of the cogeneration system in case 3.

$$R_{conv,w-p} = \frac{1}{h_w(2\pi(r_{p,o} + e)L)} \quad (14)$$

For case 5, Fig. 8 shows a cross sectional top view of the tank in which TEGs are located at the inner surface of the pipe in a direct contact with exhaust gases.

R_p , $R_{conv,w-p}$, $R_{conv,w-w}$, R_{wall} and $R_{conv,air}$ are as the reference case 1, whereas R_{TEG} and $R_{conv,i}$ are:

$$R_{TEG} = \frac{\ln \left[\frac{r_{p,i}}{r_{p,i}-e} \right]}{2\pi k_{TEG}L} \quad (15)$$

$$R_{conv,i} = \frac{1}{h_g(2\pi(r_{p,i} - e)L)} \quad (16)$$

For case 6, Fig. 9 shows the top cross sectional view in which four layers of TEGs are shown, located at the inner, and outer surface of the pipe and at the inner, and outer surface of the tank.

R_p and R_{wall} are as the reference case 1, whereas $R_{conv,i}$, R_{TEG} , $R_{conv,w-p}$, $R_{conv,w-w}$ and $R_{conv,air}$ are:

$$R_{conv,i} = \frac{1}{h_g(2\pi(r_{p,i} - e)L)} \quad (17)$$

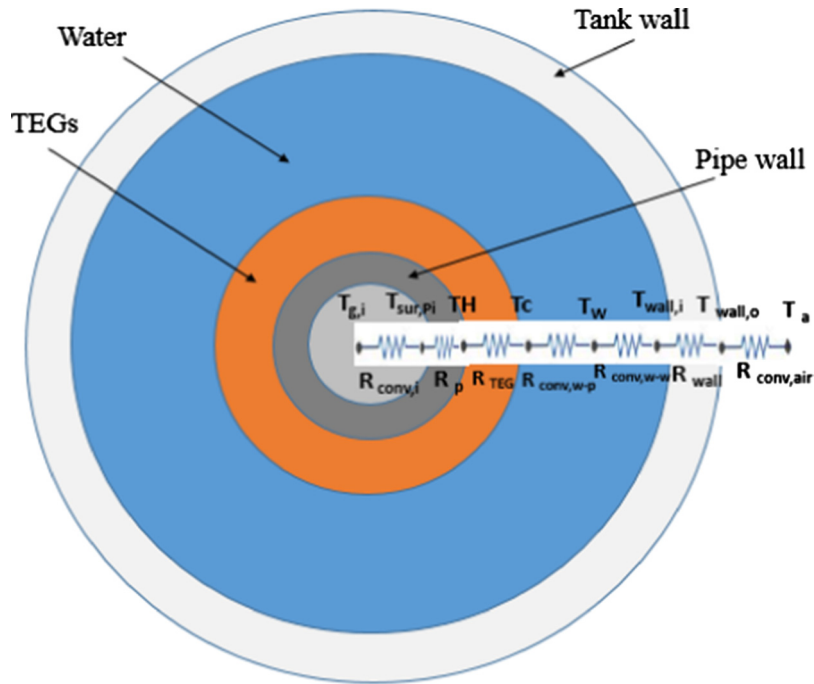


Fig. 7. Top cross sectional view of the cogeneration system in case 4.

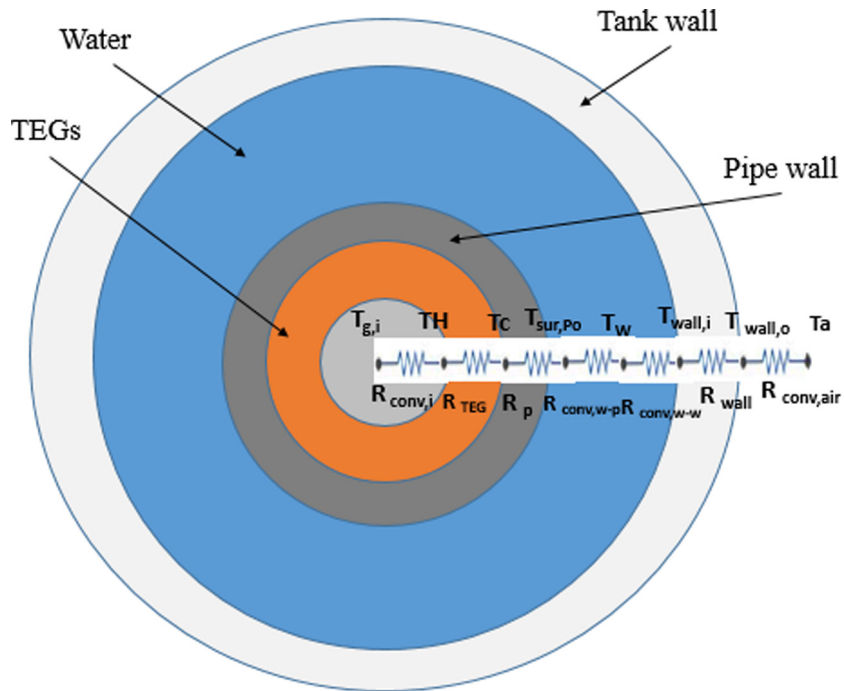


Fig. 8. Top cross sectional view of the cogeneration system in case 5.

$$R_{TEG1} = \frac{\ln \left[\frac{r_{p,i}}{r_{p,i}-e} \right]}{2\pi k_{TEG}L}$$

$$(18) \quad R_{conv,w-w} = \frac{1}{h_w(2\pi(r_{w,i} - e)L)} \tag{21}$$

$$R_{TEG2} = \frac{\ln \left[\frac{r_{p,o}+e}{r_{p,o}} \right]}{2\pi k_{TEG}L}$$

$$(19) \quad R_{TEG3} = \frac{\ln \left[\frac{r_{w,i}}{r_{w,i}-e} \right]}{2\pi k_{TEG}L} \tag{22}$$

$$R_{conv,w-p} = \frac{1}{h_w(2\pi(r_{p,o} + e)L)}$$

$$(20) \quad R_{TEG4} = \frac{\ln \left[\frac{r_{w,o}+e}{r_{w,o}} \right]}{2\pi k_{TEG}L} \tag{23}$$

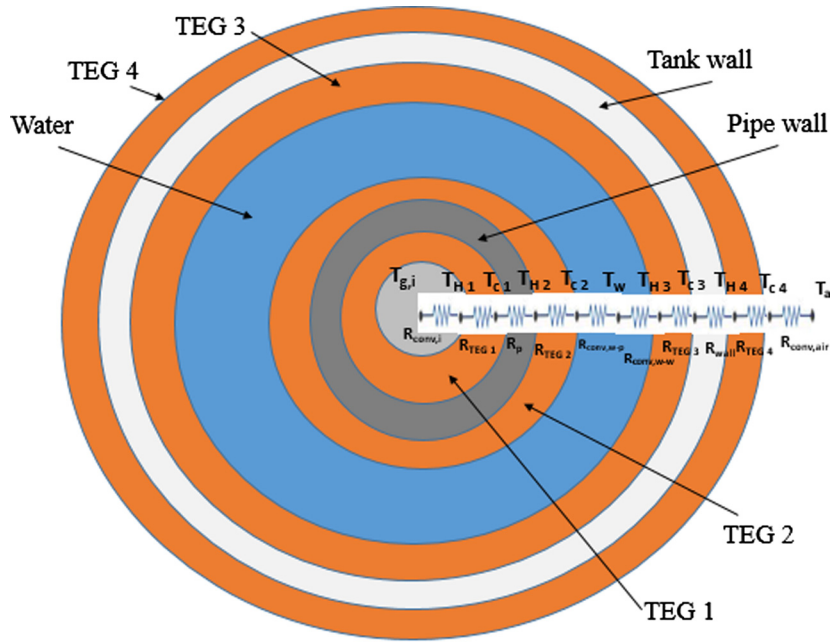


Fig. 9. Top cross sectional view of the cogeneration system in case 6.

$$R_{conv,air} = \frac{1}{h_a(2\pi(r_{w,o} + e)L)} \quad (24)$$

where $r_{p,i}$, $r_{p,o}$, $r_{w,i}$ and $r_{w,o}$ are the inner, outer radius of the pipe and inner, outer radius of the tank wall respectively, e is the thickness of the thermoelectric generator, h_g , h_w , and h_a are the convection heat transfer coefficient of the exhaust gases, water and air respectively.

Heat flow rate is constant over the system then the temperature at each point can be calculated:

$$T_{(n)} = T_{(n-1)} - qR_{(n)} \quad (25)$$

where “n” is the layer number measured from the exhaust gases to the air. Then the hot and cold temperature at the sides of the TEG is estimated, this allows the calculation of the power output of one TEG:

$$\left(\frac{P}{\Delta T^2}\right)_{Ref} = \left(\frac{P_{1TEG}}{\Delta T^2}\right) \quad (26)$$

$$P_{1TEG} = \left(\frac{P}{\Delta T^2}\right)_{Ref} \Delta T^2 \quad (27)$$

where P_{1TEG} is the output power of one TEG, ΔT is the temperature difference between the heat source and heat sink of the TEG, and $\left(\frac{P}{\Delta T^2}\right)_{Ref}$ is given by the manufacturer of the TEG.

In order to obtain the number of TEGs available, area of TEG should be calculated in addition to the area of the wall that the TEGs are located on ($A_{TEG\ wall}$), then number of TEGs (N_{TEG}) will be:

$$N_{TEG} = \frac{A_{TEG\ wall}}{A_{TEG}} \quad (28)$$

Then the total power generated (P_{total}) is:

$$P_{Total} = N_{TEG} \cdot P_{1TEG} \quad (29)$$

4. Case study, results and discussion

A case study was considered in order to check the change in the water temperature and the power generated by changing the

thermoelectric generator location, in which a heat recovery system form exhaust gases of a chimney in Lebanon has been studied. The study is composed of two stages experimental and analytical.

4.1. Experimental data

The part related to the parameters of the exhaust gases was estimated experimentally, in which an experiment was done in order to measure the temperature of the exhaust gases that flows out from the chimney. Fig. 10 shows a Diesel chimney used in the experiment.

The ambient air temperature and the exhaust gases temperature was measured using a K type thermocouple. The temperature of the exhaust gases fluctuates during the experiment (Fig. 11) having an average value of 300 °C.

4.2. Analytical study

It should be noted that the temperature of the exhaust gases was estimated experimentally. The recovery system parameters utilized in the experiment are summarized in Table 3.

About 187 L of water are contained in an iron tank. The pipe is formed from copper to enhance the heat transfer between exhaust gases and water or TEGs. The thermoelectric generator used is “TEG1-12611-8.0” 56*56 mm. It should be noticed that this study was carried out on a specific type of TEG. However when the type of TEG is changed, the thermal resistance, the power produced, the water temperature, the figure of merit, and the energy conversion efficiency will change. The exhaust gases temperature is measured directly before the gases enter the recovery tank, in which this temperature is taken as average temperature after waiting the system to stabilize (temperature fluctuates over time). Table 4 shows the main results by applying the equations listed above in the previous section.

By checking the total resistance in each case it shows that R_{total} is lowest when there is no TEG, and it starts to increase by adding TEGs. Also it increases when the location of the TEG become nearer to the exhaust gases. And it is highest when the thermoelectric generators are added in all locations (case 6). This increase in total



Fig. 10. Diesel chimney used in the experiment.

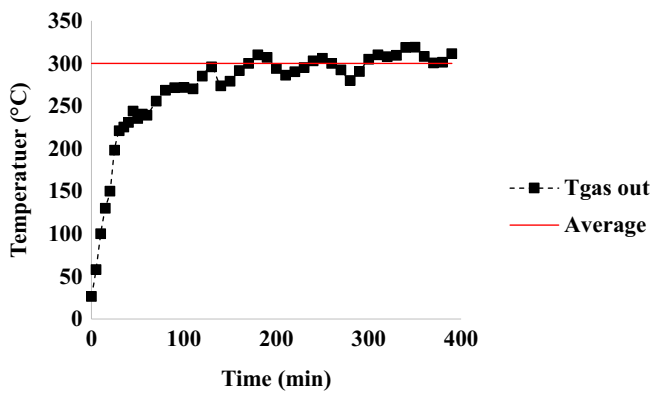


Fig. 11. Exhaust gases outlet temperature from chimney.

Table 3
Main parameters used in this study [60,61].

Parameter	Value	Unit
$r_{p,i}$	0.049	m
$r_{p,o}$	0.05	m
L	1	m
$r_{w,i}$	0.249	m
$r_{w,o}$	0.25	m
h_g	85	W/m ² K
h_{water}	300	W/m ² K
h_{air}	50	W/m ² K
k_p	401	W/m K
k_{wall}	80	W/m K
k_{TEG}	1.4	W/m K
T_g	300	°C
T_a	25	°C
e	0.005	m
$P/\Delta T^2$	0.0002	W/K ²
A_{TEG}	0.0031	m ²

resistance led to a decrease in heat flow rate from exhaust gases to the ambient, this means that lower energy is being dissipated to the environment. This change in total resistance led to a change in temperature distribution over the system as shown in Table 5 below.

It should be noted that since the temperature of the exhaust gases are assumed to be constant over the length of the tank this results will be the same along the length of the tank. Fig. 12 shows the temperature profile over the cross section of the tank. It shows that the temperature decrease rapidly at the pipe, this is due to the low convection heat transfer coefficient of gases at a small distance (radius of the pipe 25 mm). However in water, temperature decreases as it become far away from the pipe but with low slope which is due to the high convection heat transfer coefficient of water (300 W/m² K).

The main gains from this hybrid heat recovery system are the water temperature and the output power generated. Table 5 above shows that water temperature has increased in case 2, and 3 more than in the reference case 1 because of the heat trapped inside the tank by adding more thermal resistance at the wall of the tank. Besides the water temperature has increased more when the TEGs are located in the inner wall of the tank (case 3). While when the TEGs are located on the inner or outer surface of the pipe (cases 4 or 5) the water temperature becomes less than in cases 1, 2 and 3, this is due to the thermal energy absorbed by the TEGs before being given to the water. Also, by locating the TEGs in pipe's outer surface (case 5) the temperature of water is higher than when TEGs are located at the inner surface of the TEGs (case 4). This means that when the TEGs are inside the pipe (in a direct contact with the exhaust gases) they absorb more thermal energy than when they are in an indirect contact (case 2, 3, and 4). In the last case (case 6) water temperature is relatively in the range of case 4 and 5. Fig. 13 shows the water temperature in each case, the maximum water temperature achieved is 97 °C in case 3 and the minimum temperature is 76 °C in case 5. The water temperature varied in a relatively high range (about 20 °C) when the TEGs location have been changed.

Regarding the power generated by TEGs, Eq. (27), it shows that the power is directly proportional to the square of the temperature difference between the heat source and sink of the TEGs. Then as the temperature difference increases, power produced increases. Table 4 above shows that when the TEGs are in the inner surface of the tank it involves more temperature difference than when it is in the outer surface. However it implies maximum temperature difference when the TEGs are located in the inner surface of the pipe (direct contact with exhaust gases). Also it shows that the temperature difference is higher when the TEGs are located in the pipe surfaces (inner or outer) more than when the TEGs are located at the tank surfaces. For the last case (case 6) the temperature difference decreases as the TEGs location become far away from the exhaust gases.

The maximum power produced per one TEG is on the fifth case, but the maximum total power is for case 6. It should be noted that fifth case has much less TEGs than second, third, and fourth case (shown in Table 4 above) but produces higher power output. Regarding case 6 the power produced per one TEG is less than the power produced in the other cases at each stage, but the total power produced is higher than the other cases. Fig. 14 shows the power generated per one TEG, on which obviously appears that the maximum power generated by one TEG is in case 5 (0.35 W). This means that the TEGs are maximally utilized in case 5 which increases the efficiency of the thermoelectric generator.

Fig. 15 shows the total power produced by thermoelectric generators in each case.

The maximum power produced is 52 W in case 6 and minimum power is in case 2 (6.8 W). Comparing cases 2 and 3, case 3 produces about 4% more power than case 2. While in case 5 the power produced increases about 5% compared to case 4. And comparing cases 2–3 with 4–5, cases 4–5 produces about 400% more power than cases 2–3 can produce.

Table 4
Main results obtained in the six studied cases, temperatures expressed in °C.

Case number	R_{total} (°C/W)	q (W)	T_w (°C)	TEG location	ΔT	Number of TEG	Power of 1 TEG (W)	P_{total} (W)	
Case 1	0.063	4317	89	Null	0	0	0	0	
Case 2	0.065	4186	96	Outer tank's surface	9.4	385	0.0177	6.8	
Case 3	0.066	4163	97	Inner tank's surface	9.6	383	0.0180	7.1	
Case 4	0.073	3738	81	Outer pipe's surface	40	101	0.32	33.1	
Case 5	0.080	3426	76	Inner pipe's surface	42	99	0.35	34.8	
Case 6	0.094	2910	81	Inner pipe's surface	36	99	0.25	25.1	52
				Outer pipe's surface	32	101	0.19	20.1	
				Inner tank's surface	6.7	383	0.009	3.5	
				Outer tank's surface	6.6	385	0.008	3.3	

Table 5
Temperature distribution over the system and power produced by the TEGs.

Case 1	$T_{g,i}$ 300	$T_{sur,Pl}$ 135	$T_{sur,Po}$ 134	T_w 89	$T_{wall,i}$ 80	$T_{wall,o}$ 79	T_a 25				
Case 2	$T_{g,i}$ 300	$T_{sur,Pl}$ 140	$T_{sur,Po}$ 139	T_w 96	$T_{wall,i}$ 87	T_H 86	T_c 77	T_a 25			
Case 3	$T_{g,i}$ 300	$T_{sur,Pl}$ 141	$T_{sur,Po}$ 140	T_w 97	T_H 88	T_c 79	$T_{wall,o}$ 78	T_a 25			
Case 4	$T_{g,i}$ 300	$T_{sur,Pl}$ 157	T_H 156	T_c 116	T_w 81	$T_{wall,i}$ 73	$T_{wall,o}$ 72	T_a 25			
Case 5	$T_{g,i}$ 300	T_H 154	T_c 113	$T_{sur,Po}$ 112	T_w 76	$T_{wall,i}$ 69	$T_{wall,o}$ 68	T_a 25			
Case 6	$T_{g,i}$ 300	$T_{H 1}$ 176	$T_{c 1}$ 141	$T_{H 2}$ 140	$T_{c 2}$ 109	T_w 81	$T_{H 3}$ 75	$T_{c 3}$ 68	$T_{H 4}$ 67	$T_{c 4}$ 61	T_a 25

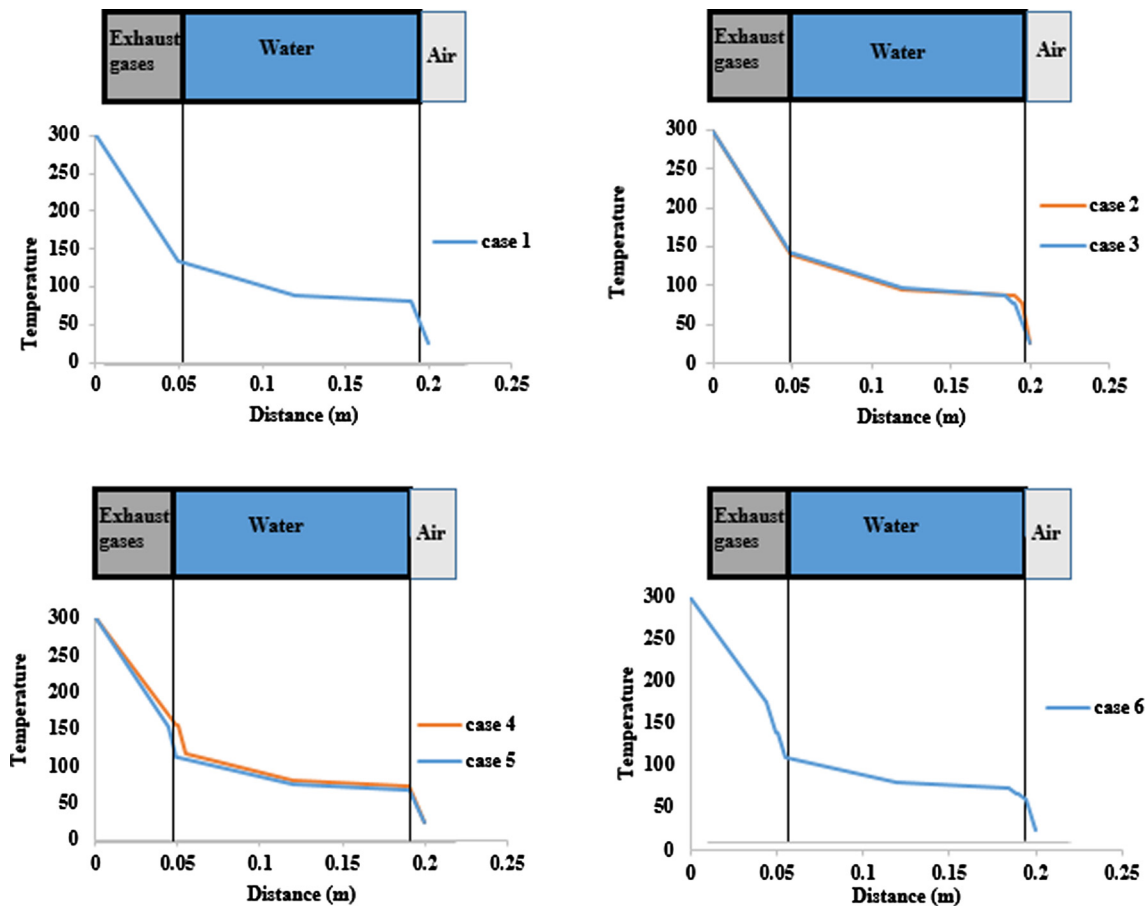


Fig. 12. Temperature profile over the cylindrical tank.

Regarding the thermal energy lost with the surrounding, Fig. 16 shows that case 5 has the lowest outer tank wall temperature, if case 6 is excluded from comparison. For the 6th case the tempera-

ture of the outer wall of the tank is lower than all the previous cases, due to the energy absorption by the multi-stages of TEGs. Comparing cases 2, 3, 4, and 5, case 5 provides the lowest thermal



Fig. 13. Water temperature variation in each case.

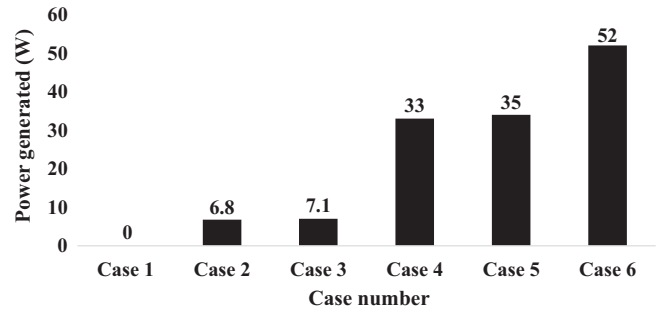


Fig. 15. Total power generated by thermoelectric generators.

energy loss. This made case 5 with the lowest thermal energy lost and highest power produced by TEGs compared to cases 2, 3, and 4.

5. Economic and environmental concerns

It should be noted that locating the TEGs at the surface of the pipe would decrease the cost 75% compared to locating TEGs at the tank's surfaces (number of TEGs located at the pipe is about 1/4 number of TEGs located at the tank). Fig. 17 shows the power generated and the cost of TEGs at each stage, knowing that the cost of one TEG is given by the manufacturer (20 \$/1 TEG) [61].

As shown in Fig. 17, if the water temperature is the major requirement, then case 3 is the best. However, if the power generated is the major requirement without taking into consideration the cost, case 6 is the best. On the other hand, if the cost and power are major requirements then case 5 is the best since case 5 has a relatively high water temperature, high power generated, low thermal energy losses with ambient air, and low cost of thermoelectric generators compared to case 2, 3, and 4.

For a cost-effective heat recovery system, case 5 is the best choice since it produces relatively high power with low number of TEGs (low cost). Also water temperature is relatively acceptable compared to the maximum water temperature and it has the lowest thermal energy losses.

Then, the total price of the system is calculated as the sum of the price of iron tank, the price of the copper pipe and the assembly process in addition to the price of the thermoelectric generators.

The price of the iron used to make the tank is calculated by the equation below:

$$\text{price of iron} = m_{\text{iron}} \times \text{price of 1 kg of iron} \quad (30)$$

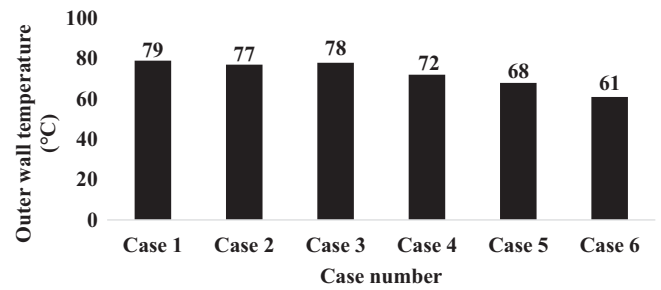


Fig. 16. Outer wall temperature in each case.

where m_{iron} is the mass of iron. The price of 1 kg of the iron used is 3 USD. The mass of the iron is estimated as follows:

$$m_{\text{iron}} = V_{\text{iron}} \rho_{\text{iron}} \quad (31)$$

where V_{iron} and ρ_{iron} are the volume and density of iron respectively. The density of iron is 7850 kg/m³. Eq. (32) shows how to calculate the volume of iron:

$$V_{\text{iron}} = \pi L(r_{w,o}^2 - r_{w,i}^2) + 2\pi r_{w,o}^2 l \quad (32)$$

where l is the thickness of the iron sheet at the upper and lower part of the tank. By applying the previous equations, $V_{\text{iron}} = 0.0024 \text{ m}^3$, $m_{\text{iron}} = 18.5 \text{ kg}$, and the total cost of the iron used is 56 \$.

Then the price of the copper can be estimated by the following equations:

$$\text{price of copper} = m_{\text{copper}} \times \text{price of 1 kg of copper} \quad (33)$$

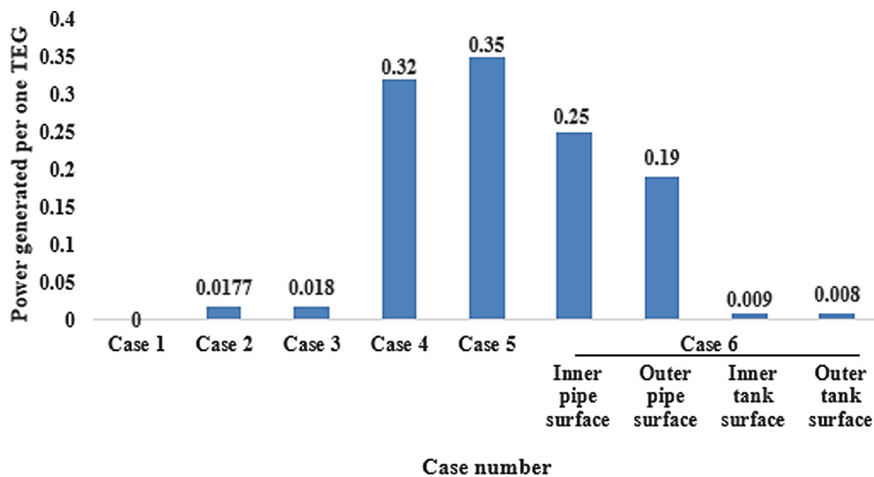


Fig. 14. Power generated per one TEG in the six studied cases.

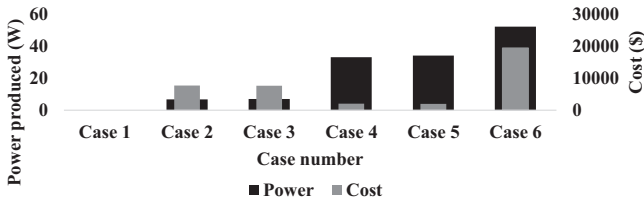


Fig. 17. Total power generated and total cost of the TEGs in each case.

$$m_{copper} = V_{copper} \rho_{copper} \tag{34}$$

$$V_{copper} = \pi L (r_{p,o}^2 - r_{p,i}^2) \tag{35}$$

where m_{copper} , V_{copper} and ρ_{copper} are the mass, volume, and density of copper respectively. The density of copper is 8940 kg/m³, and the price of 1 kg of copper used is 12 USD. By applying Eqs. (33)–(35), $V_{copper} = 0.0003 \text{ m}^3$, $m_{copper} = 2.8 \text{ kg}$, and the total cost of the copper used is 34 \$.

The assemblage process consists of rolling the iron and copper sheets as cylinders in addition to welding required gathering all the parts together. This process costs 80 \$. Then the total price of the system without the thermoelectric generators is 170 \$.

Table 6
Total price of the system in each case in USD.

Case number	Price (\$)
Case 1	170
Case 2	7870
Case 3	7830
Case 4	2190
Case 5	2150
Case 6	19530

Table 6 shows the total price of each case, in which the cost of the TEGs is added to the cost of the system without thermoelectric generators.

In order to calculate how much energy this system saves, then how much money it saves, the electric power required to heat such amount of water is calculated for a specified temperature rise. This electric power is then added to the power generated by TEGs. Fig. 18 shows a tree in which the procedure of calculating the money saving is shown.

The volume of the water found in the system is 0.187 m³ calculated by the following equation:

$$V_{water} = \pi L (r_{w,i}^2 - r_{p,o}^2) \tag{36}$$

where V_{water} is the volume of the water in the tank.

Thermal energy required Q to heat the water is calculated by:

$$Q = \rho V_{water} C_{p_{water}} \Delta T \tag{37}$$

where $C_{p_{water}}$ and ΔT are the specific heat of water at constant pressure, and the temperature rise of water respectively. Then applying Eq. (37), with $C_{p_{water}} = 4.187 \text{ kJ/kg K}$, and $\Delta T = 70 \text{ }^\circ\text{C}$, Q is obtained equal to 54.6 kJ.

A conventional water heater is used with an energy efficiency of 80%. Then the electric energy consumption for heating this amount of water is estimated by the following equation:

$$\eta = \frac{Q_{thermal}}{EEC} \tag{38}$$

$$EEC = \frac{Q_{thermal}}{\eta} \tag{39}$$

where η , EEC are the efficiency and the electric energy consumption. Then the consumed electric energy to heat the water is 68278 kJ, or 19 kWh to heat 0.187 m³ of water with 70 °C temperature rise.

Fig. 19 shows the variation of energy consumption and its equivalent cost by varying the number of times the water was

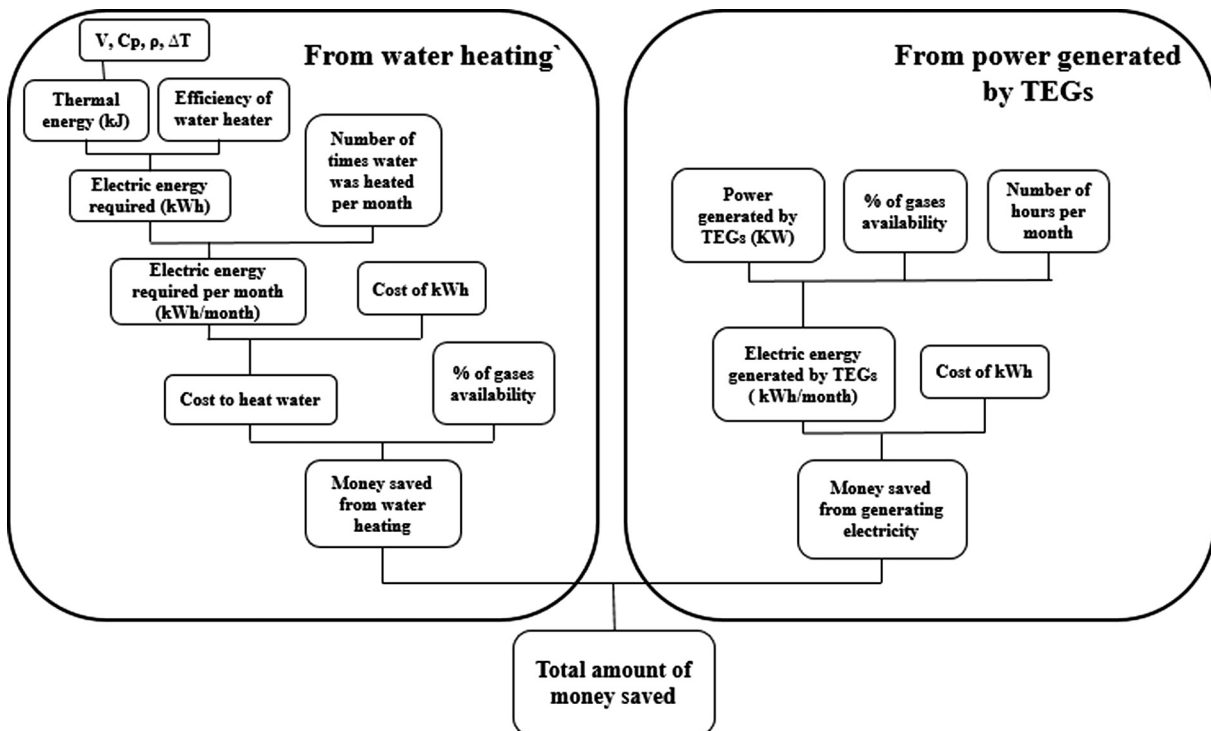


Fig. 18. Saved money calculation procedure schematic.

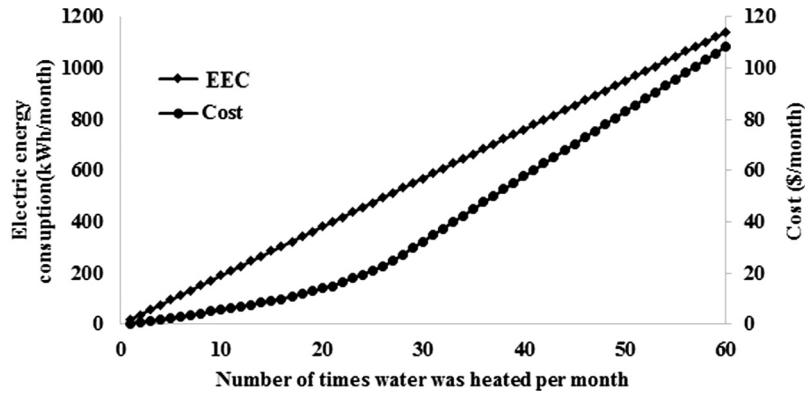


Fig. 19. Electric Energy required and its equivalent cost per month for different number of times water was heated.

Table 7
Cost of 1 kW h in Lebanon.

Electric rates in one month	Cost (\$/kW h)
0–99 kW h/month	0.023
100–299 kW h/month	0.037
300–399 kW h/month	0.053
400–499 kW h/month	0.08
>500 kW h/month	0.133

heated in one month, where the price of the electric energy is calculated according to the kW h prices in Lebanon illustrated in Table 7.

It should be noted that if the exhaust gases are always available then the amount of money saved from heating water is exactly the cost of the electric power required to heat the water. However if the exhaust gases are not always available then the amount of money saved from heat water $MS_{water\ heating}$ is:

$$MS_{water\ heating} = P_r \times C_{electric\ power\ required\ to\ heat\ water} \quad (40)$$

where P_r and $C_{electric\ power\ required\ to\ heat\ water}$ are the percentage of availability of gases to run the hybrid heat recovery system and the cost of the electric energy required to heat water respectively. Regarding the exhaust gases presence, it was important to take into consideration the availability of this gases (P_r) due to the fact that sometimes the chimney would be off. Fig. 20 shows the money saved from water heating for different percentages of gas availability.

It should be noted the high amount of money saved from heat water using the hybrid heat recovery system (more than 100 \$/month). This is due to the high electric energy consumption for heating water and it is the main source of high electric bills.

In order to estimate the total amount of money saved, which is the amount of money saved from heating the water and the price

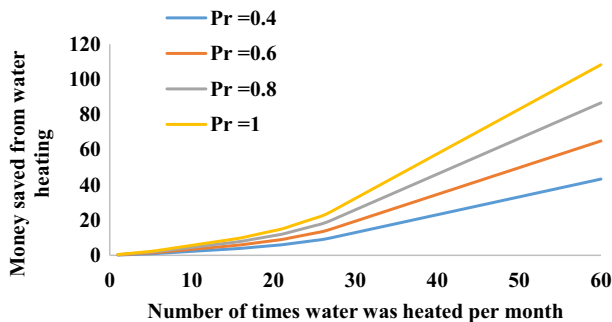


Fig. 20. Money saved from water heating process over different gases availability percentage.

of the generated electricity via TEGs, the electric energy generated per month by the thermoelectric generators $E_{generated/month}^{TEG}$ should be calculated as below:

$$E_{generated/month}^{TEG} (kW\ h/month) = P_r \times P_{generated}^{TEG} (kW) \times \left(\frac{30\ days}{month}\right) \times \left(\frac{24\ hours}{day}\right) \quad (41)$$

where $P_{generated}^{TEG}$ is the total power generated by thermoelectric generators in kW.

Fig. 21 shows the total power generated by the TEGs over one month for each case over various gases availability percentage.

The cost of the electric energy generated from the TEGs in each case is shown in Fig. 22. Assuming that the electric energy

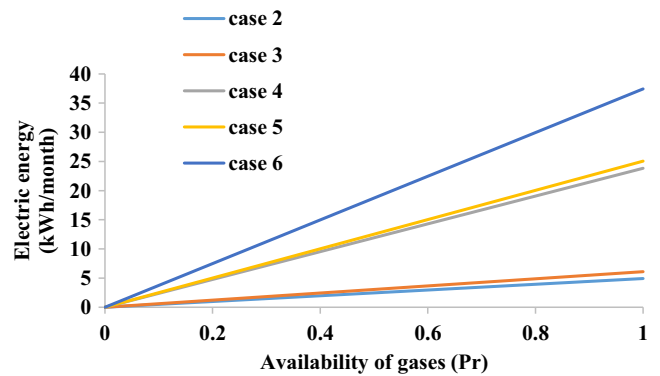


Fig. 21. Electric energy generated monthly by TEGs.

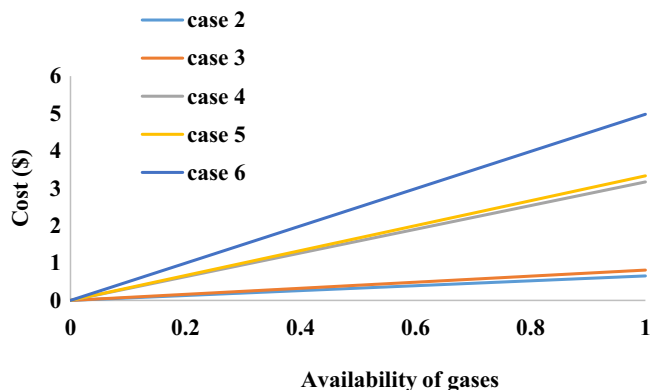


Fig. 22. Cost of generated electric energy generated by TEGs.

consumption over the month is always greater than 500 kW h, then the price of 1 kW h from the TEGs is 0.133 \$/kW h. The cost of the electric energy generated by TEGs $C_{electric\ energy}^{TEG}$ is calculated as follows:

$$C_{electric\ energy}^{TEG} = E_{generated/month}^{TEG} (kW\ h/month) \times C_{1\ kW\ h} \quad (42)$$

where $C_{1\ kW\ h}$ is the cost of one kW h expressed in \$/kW h.

The total amount of money saved MS_{total} by the hybrid heat recovery system from heating water and generating electricity is:

$$MS_{total} = MS_{water\ heating} + C_{electric\ energy}^{TEG} \text{ at constant } P_r \quad (43)$$

Fig. 23 shows the total amount of money saved with $P_r = 1$, with respect to the number of times water was heated per month for each of the six cases.

The total amount of money saved is approximately the same in the six cases which means that changing the location of TEGs have little influence in total money saved per month, due to the high cost of heat water compared to the cost of generating electricity.

The payback period Pbp of the hybrid heat recovery system is calculated using Eq. (44), it shows that it will be variable with respect to how much water is heated per month and the percentage of gases availability:

$$Pbp = \frac{HHRSC}{MS_{total}} \quad (44)$$

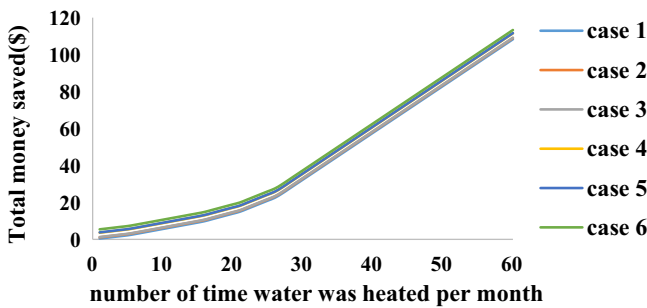


Fig. 23. Total amount of money saved at $P_r = 1$.

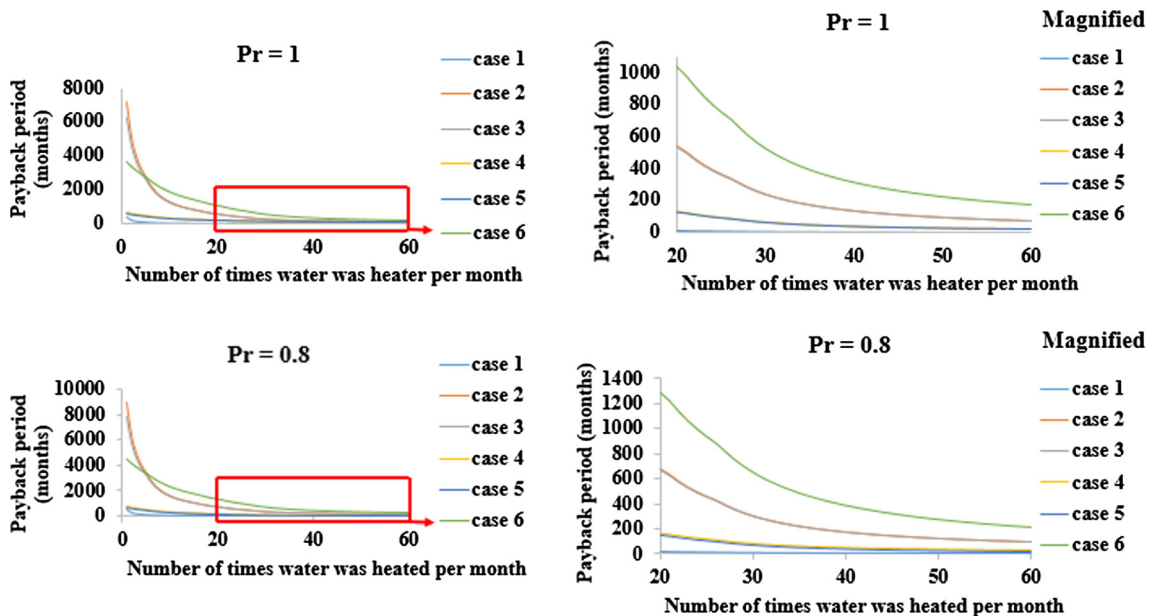


Fig. 24. Payback period for the hybrid heat recovery system for percentage availability of gases $P_r = 1$ and 0.8.

where $HHRSC$ is the total cost of the hybrid heat recovery system in each case. Fig. 24 shows the payback period of each case for different exhaust gases availability percentage.

It should be noted that if the exhaust gases are always available and comparing the hybrid heat recovery system cases, case 5 have a very good payback period of 1 year and 8 months for a 60 times of water heating. And if the water was heated 30 times the payback period is extended to about 5 years. Case 6 requires the highest payback period due to the high price of the system, mainly TEGs. It requires about 15 years to payback its cost, which is high for a residential application.

Regarding the environmental concern, heating water and producing electricity from the hybrid heat recovery system will lead to reduce the emissions of CO_2 gases resulted from burning fuel to obtain the electric power required. In order to find the reduced amount of CO_2 , the equivalent electric power reduced by water heating and the electric power produced by the TEGs is calculated. Fig. 25 shows the total power saved $P_{electrical\ total}$ which is calculated using Eq. (45). It is necessary to remind that Fig. 19 shows the electric energy saved by water heating process and Fig. 21 shows the electric energy produced by TEGs:

$$P_{electrical\ total} = P_{reduced/month}^{water\ heating} + P_{generated/month}^{TEGs} \text{ at constant } P_r \quad (45)$$

where $P_{reduced/month}^{water\ heating}$ is the electric energy saved by using the heat recovery system from the water heating.

About 0.47 kg of CO_2 is released for producing one kW h in Lebanon. This high amount of CO_2 released is due to the lack of filtering and flue gases treatment. Also it should be noted that the power grid is not 100% efficient then the power station should produce more power to transmit the required power. About 7.5% of the electricity generated is being dissipated by the power grid. Then the total power produced by the power station $P_{produced}^{power\ station}$ is:

$$P_{produced}^{power\ station} = P_{delivered} + 0.075P_{delivered} \quad (46)$$

where $P_{delivered}$ is the power delivered to the home. Then the total power saved P_{saved}^{total} is:

$$P_{saved}^{total} = (1 + 0.075)P_{electrical\ total} \quad (47)$$

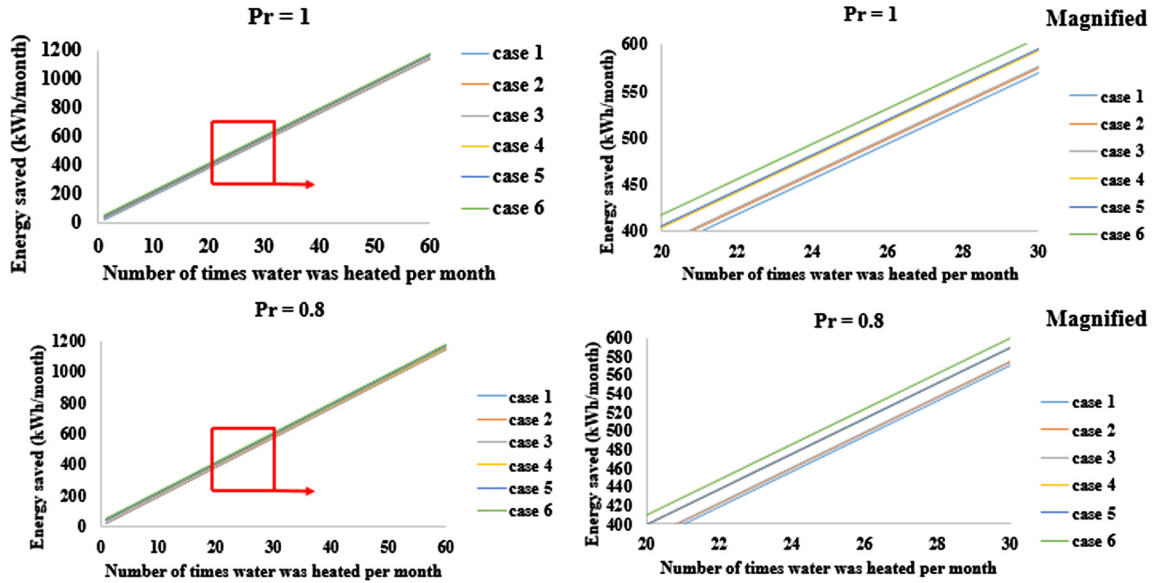


Fig. 25. Electric energy saved monthly for different gases availability percentage for percentage availability of gases $P_r = 1$ and 0.8.

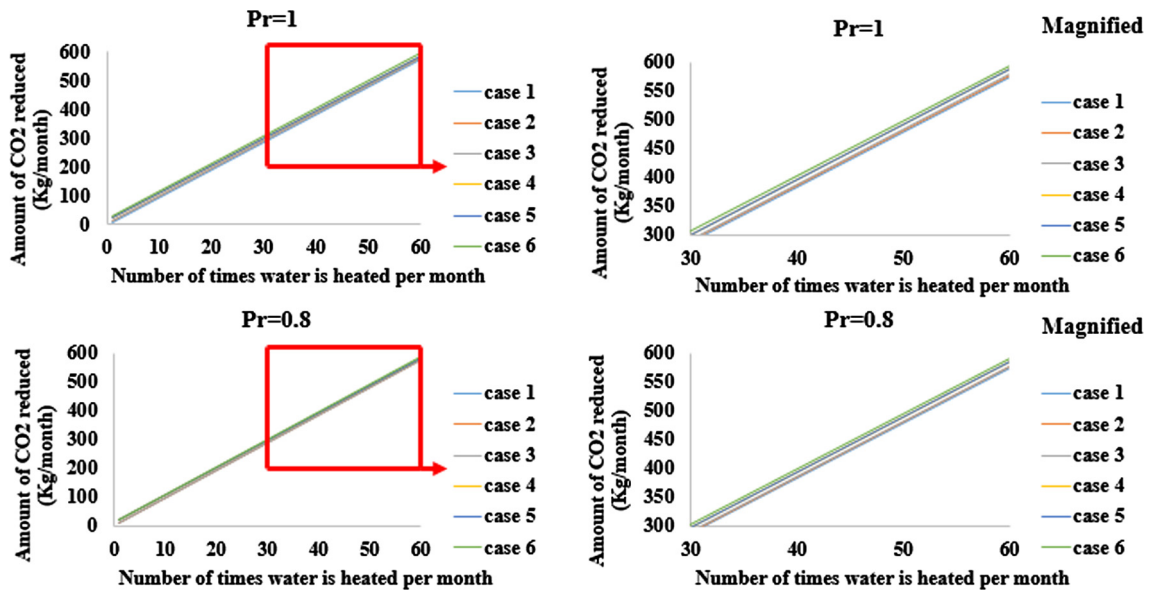


Fig. 26. Amount of CO₂ reduced by utilizing the hybrid heat recovery system monthly.

Then the reduced amount of CO₂ released $M_{CO_2}^{reduced}$ (Kg/month) is:

$$M_{CO_2}^{reduced} (kg/month) = P_{saved}^{total} (kW h/month) \times M_{CO_2}^{released} (kg/kW h) \quad (48)$$

where $M_{CO_2}^{released}$ is the mass of the CO₂ gas released for producing one kW h of electricity.

Fig. 26 shows the reduced amount of CO₂ when using the hybrid heat recovery system at different gas availability percentages.

It is shown that more than half of tons of CO₂ can be reduced monthly and mainly by the heating of water, since heating water requires high power. It could reduce about 0.6 tons of CO₂ if case 6 is utilized. The effect of changing the location of TEGs is relatively low in this case which is due to the low power produced by TEGs. Such system is capable to reduce 6 tons of CO₂ gases released to the environment yearly in Lebanon.

6. Conclusion

Heat recovery process is an advanced way for benefiting from dissipated energy. Many systems and technologies are still under study and require more advanced researchers. This paper deals with a hybrid heat recovery system used to recover heat from exhaust gases in order to cogenerate domestic hot water and to produce electricity via thermoelectric generators using domestic thermoelectric cogeneration heat recovery system (DTCHRS).

The effect of changing the location of the thermoelectric generators is studied by varying TEGs from the outer wall of the tank to its inner wall or to the outer wall of the exhaust gases pipe or to its inner wall, or even for having TEGs at all walls. Water temperature and power produced by thermoelectric generators are studied by applying a thermal modeling to a case study at steady state.

The following conclusions are drawn:

1. Locating TEGs at the wall of the tank provides higher water temperature but lower power produced (case 2 and 3). However, when TEGs are located at the pipe (case 4 and 5), high power is produced but relatively low water temperature compared to case 2 and 3. When TEGs are located at all the walls, the overall power produced is the highest and the water temperature becomes the lowest compared to other cases.
2. Cases 2 and 3 produced about 97 °C domestic hot water. However, these two configurations correspond to a low total power production (about 7 W) making them more suitable for water heating.
3. Cases 4 and 5 produced about 80 °C hot water along with 33 W of electricity generated by TEGs. The temperature of water is high but less than cases 2 and 3 and the power produced is higher than cases 2 and 3.
4. The maximum total power produced (52 W) is generated in configuration 6 with a high water temperature (81 °C). However the main limitation of this configuration is its high cost which is resulted from the high number of TEGs required (about 1000 TEGs).
5. Locating TEGs at the tank wall is more costly compared to locating them at the pipe (more TEGs are required). Then case 5 is a cost-effective heat recovery process compared to other cases if the cost is a major requirement. However if high water temperature is required then case 3 is the best. And if the cost is not the major requirement then case 6 is the better choice.
6. The economic study shows a best payback period for case 5 for which it needs 1 year and 8 months to payback the cost of the system. And as for the environmental study, it is shown that varying the location of the TEGs does not highly affect the reduced amount of CO₂ gases released, because of the low energy produced by TEGs compared to the energy gained by heating the water. Also it exhibits the fact that 6 tons of CO₂ can be reduced yearly by using the hybrid heat recovery system.
7. This system can be categorized as an indirect heat storage system. It can be transferred to a direct heat storage system by replacing water with energy storage materials (Phase change material). Moreover, it can be a combined system in which a layer or capsules of energy storage materials can be added to the system with the presence of water.

References

- [1] A. Herez, M. Ramadan, B. Abdulhay, M. Khaled, Short review on solar energy systems, in: AIP Conference Proceedings, 1758, Issue 1, 2016. <http://aip.scitation.org/doi/abs/10.1063/1.4959437>.
- [2] M. Ramadan, M. Khaled, H.S. Ramadan, M. Becherif, Modeling and sizing of combined fuel cell-thermal solar system for energy generation, Int. J. Hydrogen Energy. <http://dx.doi.org/10.1016/j.ijhydene.2016.08.222>.
- [3] A. Herez, M. Khaled, R. Murr, A. Haddad, H. Elhage, M. Ramadan, Using geothermal energy for cooling - parametric study, Energy Procedia 119 (2017) 783–791.
- [4] A. El Mays, R. Ammar, M. Hawa, M. Abou Akroush, F. Hachem, M. Khaled, M. Ramadan, Improving photovoltaic panel using finned plate of aluminum, Energy Procedia 119 (2017) 812–817.
- [5] F. Hachem, B. Abdulhay, M. Ramadan, H. El Hage, M. Gad El Rab, M. Khaled, Improving the performance of photovoltaic cells using pure and combined phase change materials - Experiments and transient energy balance, Renewable Energy 107 (July 2017) 567–575.
- [6] A. El Mays, R. Ammar, M. Hawa, M. Abou Akroush, F. Hachem, M. Khaled, M. Ramadan, Using phase change material in under floor heating, Energy Procedia 119 (2017) 806–811.
- [7] M. Khaled, M. Ramadan, H. El Hage, Innovative approach of determining the overall heat transfer coefficient of heat exchangers - Application to cross-flow water-air types, Appl. Therm. Eng. 99 (25) (April 2016) 1086–1092.
- [8] H. Jaber, M. Khaled, T. Lemenand, R. Murr, J. Faraj, M. Ramadan, Triple domestic heat recovery system thermal modeling and parametric study, in: Proceedings of SEEP2017, 27–30 June 2017, Bled, Slovenia.
- [9] H. Jaber, M. Khaled, T. Lemenand, J. Faraj, H. Bazzi, M. Ramadan, Effect of exhaust gases temperature on the performance of a hybrid heat recovery system, Energy Procedia 119 (2017) 775–782.
- [10] H. Jaber, M. Khaled, T. Lemenand, M. Ramadan, Short review on heat recovery from exhaust gas, in: AIP Conference Proceedings, 1758, Issue 1, 2016, 10.1063/1.4959441. <http://aip.scitation.org/doi/abs/10.1063/1.4959441>.
- [11] M. Terhan, K. Comakli, Design and economic analysis of a flue gas condenser to recover latent heat from exhaust flue gas, Appl. Therm. Eng. 100 (2016) 1007–1015, <https://doi.org/10.1016/j.applthermaleng.2015.12.122>.
- [12] M. Wei, X. Zhao, L. Fu, S. Zhang, Performance study and application of new coal-fired boiler flue gas heat recovery system, Appl. Energy 188 (2017) 121–129.
- [13] M. Sharma, O. Singh, Exergy analysis of dual pressure HRSG for different dead states and varying steam generation states in gas/steam combined cycle power plant, Appl. Therm. Eng. 93 (2016) 614–622, <https://doi.org/10.1016/j.applthermaleng.2015.10.012>.
- [14] A. Bassily, Modeling, analysis, and modifications of different GT cooling techniques for modern commercial combined cycle power plants with reducing the irreversibility of the HRSG, Appl. Therm. Eng. 53 (2013) 131–146, <https://doi.org/10.1016/j.applthermaleng.2013.01.002>.
- [15] K. Chae, X. Ren, Flexible and stable heat energy recovery from municipal wastewater treatment plants using a fixed-inverter hybrid heat pump system, Appl. Energy 179 (2016) 565–574, <https://doi.org/10.1016/j.apenergy.2016.07.021>.
- [16] M. Wei, W. Yuan, Z. Song, L. Fu, S. Zhang, Simulation of a heat pump system for total heat recovery from flue gas, Appl. Therm. Eng. 86 (2015) 326–332, <https://doi.org/10.1016/j.applthermaleng.2015.04.061>.
- [17] V. Karamarkovic, M. Marasevic, R. Karamarkovic, M. Karamarkovic, Recuperator for waste heat recovery from rotary kilns, Appl. Therm. Eng. 54 (2013) 470–480, <https://doi.org/10.1016/j.applthermaleng.2013.02.027>.
- [18] A. Mezquita, J. Boix, E. Monfort, G. Mallol, Energy saving in ceramic tile kilns Cooling gas heat recover, Appl. Therm. Eng. 65 (2014) 102–110, <https://doi.org/10.1016/j.applthermaleng.2014.01.002>.
- [19] M. Khaled, M. Ramadan, H. El Hage, Parametric analysis of heat recovery from exhaust gases of generators, Energy Procedia 75 (2015) 3295–3300, <https://doi.org/10.1016/j.egypro.2015.07.710>.
- [20] B. Fu, Y. Lee, J. Hsieh, Design, construction, and preliminary results of a 250-kW organic Rankine cycle system, Applied Thermal Engineering. 80 (2015) 339–346, <https://doi.org/10.1016/j.applthermaleng.2015.01.077>.
- [21] S. Bari, S. Hossain, Waste heat recovery from a diesel engine using shell and tube heat exchanger, Appl. Therm. Eng. 61 (2013) 355–363, <https://doi.org/10.1016/j.applthermaleng.2013.08.020>.
- [22] E. Wang, Z. Yu, H. Zhang, F. Yang, A regenerative supercritical-subcritical dual-loop organic Rankine cycle system for energy recovery from the waste heat of internal combustion engines, Appl. Energy 190 (2017) 574–590, <https://doi.org/10.1016/j.apenergy.2016.12.122>.
- [23] D. Jung, S. Park, K. Min, Selection of appropriate working fluids for Rankine cycles used for recovery of heat from exhaust gases of ICE in heavy-duty series hybrid electric vehicles, Appl. Therm. Eng. 81 (2015) 338–345, <https://doi.org/10.1016/j.applthermaleng.2015.02.002>.
- [24] Y. Lu, Y. Wang, C. Dong, L. Wang, A. Roskilly, Design and assessment on a novel integrated system for power and refrigeration using waste heat from diesel engine, Appl. Therm. Eng. 91 (2015) 591–599, <https://doi.org/10.1016/j.applthermaleng.2015.08.057>.
- [25] A. Boretti, Recovery of exhaust and coolant heat with R245fa organic Rankine cycles in a hybrid passenger car with a naturally aspirated gasoline engine, Appl. Therm. Eng. 36 (2012) 73–77, <https://doi.org/10.1016/j.applthermaleng.2011.11.060>.
- [26] R. Morgan, G. Dong, A. Panesar, M. Heikal, A comparative study between a Rankine cycle and a novel intra-cycle based waste heat recovery concepts applied to an internal combustion engine, Appl. Energy 174 (2016) 108–117, <https://doi.org/10.1016/j.apenergy.2016.04.026>.
- [27] T. Sung, K. Kim, Thermodynamic analysis of a novel dual-loop organic Rankine cycle for engine waste heat and LNG cold, Appl. Therm. Eng. 100 (2016) 1031–1041, <https://doi.org/10.1016/j.applthermaleng.2016.02.102>.
- [28] D. Lee, J. Park, M. Ryu, J. Park, Development of a highly efficient low-emission diesel engine-powered co-generation system and its optimization using Taguchi method, Appl. Therm. Eng. 50 (2013) 491–495, <https://doi.org/10.1016/j.applthermaleng.2012.06.040>.
- [29] M. Khaled, M. Ramadan, Study of the thermal behavior of multi concentric tube tank in heat recovery from chimney - Analysis and optimization, Heat Transfer Eng. J. 8 (2017) 1–11.
- [30] M. Khaled, M. Ramadan, K. Chahine, A. Assi, Prototype implementation and experimental analysis of water heating using recovered waste heat of chimneys, Case Stud. Therm. Eng. 5 (2015) 127–133, <https://doi.org/10.1016/j.csite.2015.03.004>.
- [31] M. Ramadan, M. Khaled, H. El Hage, Using speed bump for power generation - Modeling and experimental study, Energy Procedia 75 (2015) 867–872, <https://doi.org/10.1016/j.egypro.2015.07.192>.
- [32] X. Zhang, S. Yu, M. Yu, Y. Lin, Experimental research on condensing heat recovery using phase change material, Appl. Therm. Eng. 31 (2011) 3736–3740, <https://doi.org/10.1016/j.applthermaleng.2011.03.040>.
- [33] Z. Song, J. Chen, B. L. Yang, Heat transfer enhancement in tubular heater of Stirling engine for waste heat recovery from flue gas using steel wool, Appl. Therm. Eng. 87 (2015) 499–504. <http://dx.doi.org/10.1016/j.applthermaleng.2015.05.028>.

- [34] S. Niamsuwan, P. Kittisupakorn, I. Mujtaba, A newly designed economizer to improve waste heat recovery A case study in a pasteurized milk plant, *Appl. Therm. Eng.* 60 (2013) 188–199, <https://doi.org/10.1016/j.applthermaleng.2013.06.056>.
- [35] R. Soltani, I. Dincer, M. Rosen, Thermodynamic analysis of a novel multigeneration energy system based on heat recovery from a biomass CHP cycle, *Appl. Therm. Eng.* 89 (2015) 90–100, <https://doi.org/10.1016/j.applthermaleng.2015.05.081>.
- [36] M. Khaled, M. Ramadan, Heating fresh air by hot exhaust air of HVAC systems, *Case Stud. Therm. Eng.* 8 (2016) 398–402, <https://doi.org/10.1016/j.csite.2016.10.004>.
- [37] M. Ramadan, M. Gad El Rab, M. Khaled, Parametric analysis of air-water heat recovery concept applied to HVAC systems: Effect of mass flow rates, *Case Stud. Therm. Eng.* 6 (2015) 61–68, <https://doi.org/10.1016/j.csite.2015.06.001>.
- [38] M. Ramadan, T. Lemenand, M. Khaled, Recovering heat from hot drain water—Experimental evaluation, parametric analysis and new calculation procedure, *Energy Buildings* 128 (2016) 575–585, <https://doi.org/10.1016/j.enbuild.2016.07.017>.
- [39] C. Naldi, M. Dongellini, G. Morini, Summer performances of reversible air-to-water heat pumps with heat recovery for domestic hot water production, *Energy Procedia* 78 (2015) 1117–1122, <https://doi.org/10.1016/j.egypro.2015.11.068>.
- [40] L. Liu, L. Fu, Y. Jiang, Application of an exhaust heat recovery system for domestic hot water, *Energy* 35 (2010) 1476–1481, <https://doi.org/10.1016/j.energy.2009.12.004>.
- [41] N. Kumar, G. Mohan, A. Martin, Performance analysis of solar cogeneration system with different integration strategies for potable water and domestic hot water production, *Appl. Energy* 170 (2016) 466–475, <https://doi.org/10.1016/j.apenergy.2016.02.033>.
- [42] A. Ibáñez, J. Linares, M. Cledera, B. Moratilla, Sizing of thermal energy storage devices for micro-cogeneration systems for the supply of domestic hot water, *Sustain. Energy Technol. Assessments* 5 (2014) 37–43, <https://doi.org/10.1016/j.seta.2013.11.002>.
- [43] S. Hossain, S. Bari, Waste heat recovery from exhaust of a diesel generator set using organic fluids, in: 10th International Conference on Mechanical Engineering, ICME.Procedia Engineering, vol. 90, 2014, pp. 439–444. <http://dx.doi.org/10.1016/j.proeng.2014.11.753>.
- [44] S. Prabu, M. Asokan, A study of waste heat recovery from diesel engine exhaust using phase change material, *Int. J. ChemTech Res.* 8 (2015) 711–717.
- [45] Y. Najjar, A. Abubaker, A. El-Khalil, Novel inlet air cooling with gas turbine engines using cascaded waste-heat recovery for green sustainable energy, *Energy* 93 (2015) 770–785, <https://doi.org/10.1016/j.energy.2015.09.033>.
- [46] H. Gao, G. Huang, H. Li, Z. Qu, Y. Zhang, Development of stove-powered thermoelectric generators A review, *Appl. Therm. Eng.* 96 (2016) 297–310, <https://doi.org/10.1016/j.applthermaleng.2015.11.032>.
- [47] A. Montecucco, J. Siviter, A.R. Knox, Combined heat and power system for stoves with thermoelectric generators, *Appl. Energy* 185 (2017) 1336–1342, <https://doi.org/10.1016/j.apenergy.2015.10.132>.
- [48] W. He, G. Zhang, X. Zhang, J. Ji, G. Li, X. Zhao, Recent development and application of thermoelectric generator and cooler, *Appl. Energy* 143 (2015) 1–25, <https://doi.org/10.1016/j.apenergy.2014.12.075>.
- [49] J. Wang, J.Y. Wu, C. Zheng, Simulation and evaluation of a CCHP system with exhaust gas deep-recovery and thermoelectric generator, *Energy Convers. Manage.* 86 (2014) 992–1000, <https://doi.org/10.1016/j.enconman.2014.06.036>.
- [50] T. Ma, X. Lu, J. Pandit, S. Ekkad, S. Huxtable, S. Deshpande, Q. Wang, Numerical study on thermoelectric–hydraulic performance of a thermoelectric power generator with a plate-fin heat exchanger with longitudinal vortex generators, *Appl. Energy* 185(Part 2) (2017) 1343–1354, <https://doi.org/10.1016/j.apenergy.2016.01.078>.
- [51] X. Sun, X. Liang, G. Shu, H. Tian, H. Wei, X. Wang, Comparison of the two-stage and traditional single-stage thermoelectric generator in recovering the waste heat of the high temperature exhaust gas of internal combustion engine, *Energy* 77 (2014) 489–498, <https://doi.org/10.1016/j.energy.2014.09.032>.
- [52] J. Jang, Y. Tsai, Optimization of thermoelectric generator module spacing and spreader thickness used in a waste heat recovery system, *Appl. Therm. Engineering* 51 (2013) 677–689, [10.1016/j.applthermaleng.2012.10.024](https://doi.org/10.1016/j.applthermaleng.2012.10.024).
- [53] C. Lu, S. Wang, C. Chen, Y. Li, Effects of heat enhancement for exhaust heat exchanger on the performance of thermoelectric generator, *Applied Thermal Eng.* 89 (2015) 270–279, <https://doi.org/10.1016/j.applthermaleng.2015.05.086>.
- [54] E. Navarro-Peris, J. Corberan, Z. Ancik, Evaluation of the potential recovery of compressor heat losses to enhance the efficiency of refrigeration systems by means of thermoelectric generation, *Appl. Therm. Eng.* 89 (2015) 755–762, <https://doi.org/10.1016/j.applthermaleng.2015.05.086>.
- [55] H. Ma, C. Lin, H. Wu, C. Peng, C. Hsu, Waste heat recovery using a thermoelectric power generation system in a biomass gasifier, *Appl. Therm. Eng.* 88 (2015) 274–279, <https://doi.org/10.1016/j.applthermaleng.2014.09.070>.
- [56] X. Zheng, Y. Yan, K. Simpson, A potential candidate for the sustainable and reliable domestic energy generation—Thermoelectric cogeneration system, *Appl. Therm. Eng.* 53 (2) (2013) 305–311, <https://doi.org/10.1016/j.applthermaleng.2012.03.020>.
- [57] X. Zheng, C. Liu, R. Boukhanouf, Y. Yan, W. Li, Experimental study of a domestic thermoelectric cogeneration system, *Appl. Therm. Eng.* 62 (1) (2014) 69–79, <https://doi.org/10.1016/j.applthermaleng.2013.09.008>.
- [58] K. Alanne, T. Laukkanen, K. Saari, J. Jokisalo, Analysis of a wooden pellet-fueled domestic thermoelectric cogeneration system, *Appl. Therm. Eng.* 63 (1) (2014) 1–10, <https://doi.org/10.1016/j.applthermaleng.2013.10.054>.
- [59] S. Yu, Q. Du, H. Diao, G. Shu, K. Jiao, Start-up modes of thermoelectric generator based on vehicle exhaust waste heat recovery, *Appl. Energy* 138 (2015) 276–290, <https://doi.org/10.1016/j.apenergy.2014.10.062>.
- [60] F.P. Incropera, D.P. DeWitt, *Fundamentals of heat and mass transfer, sixth ed.*, John Wiley & Sons, 2007.
- [61] Tecteg, Manufacturer of thermoelectric modules, 2016, Available from <http://www.tecteg.com>.